Proc. Indian Acad. Sci. (Earth Planet. Sci.), Vol. 98, No. 4, December 1989, pp. 339–352.

Stratification and convection over Arabian Sea during monsoon 1979 from satellite data

M S NARAYANAN and B M RAO

Meteorology and Oceanography Division, Remote Sensing Area, Space Applications Centre, Ahmedabad 380053, India

MS received 8 May 1989; revised 30 September 1989

Abstract. From the temperature and moisture retrievals from satellites, two types of indices were derived: one indicating suppression of convection and the other indicating organized deep convection. Sea surface skin temperature and equivalent potential temperatures up to 500 mbar level of the atmosphere, derived from TIROS-N satellite products, are the basis of the two indices. The maps of these indices for various phases of 1979 monsoon are compared with percentage cloudiness, a product also available from TIROS-N satellite observations. Despite the various limitations of satellite soundings, it is shown that these satellite-derived indices can be used to indicate the strengths of atmospheric convection and inversion over the oceans.

Keywords. TOVS; monsoon; inversion; stability; convection; Arabian Sea.

1. Introduction

An understanding of the factors that favour and inhibit convection over the Indian Ocean and adjoining seas is important to many aspects of monsoon dynamics. Deep convection can be thought to be related to the distribution of sea surface temperature (SST) and prevailing low level winds. Evidence of thermal stratification of the summer monsoon air over the Arabian sea indicates temperature inversion in the lower atmosphere.

Two principal factors govern the generation and sustenance of both these phenomena: the atmospheric thermodynamic stability and dynamical forcing providing large scale vertical motion. The stratification of the atmosphere helps determine the initiation and subsequent development of convection as well as its vertical extent. Until the last decade the only source of information on the vertical structure of the tropical oceanic atmosphere was from the network of upper air stations over islands or during special observing upsondes/dropsondes during major global observational programmes (e.g. IIOE, FGGE/MONEX, GATE etc). Large scale climatological characteristics of atmospheric stability and their deviations have thus been non-existent.

With the advent of polar orbiting satellites with atmospheric sounding capabilities this has now become realizable. The present authors (Narayanan and Rao 1981) had earlier shown that atmospheric stratifications during monsoon can be delineated from such satellite soundings despite their poorer vertical resolutions and accuracies. Recently Khalsa and Steiner (1988) have shown the possibility of studying deep convection over the tropical Pacific from similar type of satellite observations.

In the above mentioned studies, different sets of sounding parameters were used. While one suggested an index for thermal inversion the other suggested deep convection, which are two opposite processes.

In this paper, we present the results from soundings where the two indices have been derived for the same period and geographic location to study their relative merits. We believe that with the combination of these two indices, it will be possible to quantitatively describe the strengths of convection/stratification.

2. Arabian sea low level inversion

The inversion over the Arabian sea is low (base between ~900 and 800 millibars (mbar) and strong over the western part and weakens and rises towards the west coast of India. It is not observed especially during active monsoon seasons. The presence of dry warm continental air from Africa and Arabia above the maritime air is thought to be associated with this inversion. Once this inversion is destroyed by some mechanism there is a favourable stratification for rapid release of moisture upwards leading to precipitation. Such observations have been reported from in situ data of the International Indian Ocean Experiment (IIOE) of 1963 and the Monsoon Experiment (MONEX) of 1979 by Colon (1964), Ramage (1966), Ghosh *et al* (1978), Sen and Das (1986) etc.

Although the basic accuracy and vertical resolution of the present-day meteorological satellite sensors cannot delineate the small-scale variations of temperature (Philips *et al* 1979) such as the monsoon inversions (or the trade wind inversions), we demonstrated for the first time that these features can indeed be detected from the TIROS-N derived skin temperature and the 1000–850 mbar layer mean temperature (LMT) by a simple difference procedure. We derived an index

$$\Delta T = \text{skin temperature} - (1000\text{–}850\,\text{mbar LMT}).$$

Using the observations of about 160 aircraft dropsonde profiles as ground truth (during MONEX of 1979), we found that if the index $\Delta T \leqslant 2$, it was indicative of inversion; higher values indicating non-inversion (but not necessarily convection) regions. We also showed how these inversion regions shifted to eastern regions during the break monsoon conditions and then back to western Arabian sea with the revival of monsoon. From these temperatures and simultaneous satellite-derived mid-tropospheric water vapour content, we also showed the close link between the extent of inversion regions and the convective processes with the Indian monsoon at its different phases.

3. Stability and convection over tropical oceans

The stability of the atmosphere having water vapour can be examined by the rate at which the temperature decreases with height. The equivalent potential temperature θ_e, is a conserved quantity under both dry and moist adiabatic ascents and offers the simplified measure of evaluating atmospheric stability. If saturated equivalent potential temperature (θ_{es}) of the atmosphere decreases with height, then a parcel can become positively buoyant once it becomes saturated, i.e. there is conditional

instability. This is not the most appropriate parameter for evaluating regions of the tropics that are favourable to deep convection because it is only a function of temperature lapse rate. It is especially true in the tropics that moisture can determine whether a given temperature sounding is capable of supporting deep convection.

A criterion that does take into account the vertical distribution of water vapour is convective or potential instability, can be expressed as $d\theta_e/dz < 0$.

Because the TOVS data exist only as average temperature and integrated water vapour for relatively thick layers of the atmosphere, they cannot be used to give a precise measure of atmospheric stability. Khalsa and Steiner (1988) sought a simple index that approximated the atmospheric stability representing the gross features of the profile. On the basis of evaluations of numerous tropical soundings, they suggested the following stability index (SI)

$$SI = \theta_{es}(3) - \theta_e(1).$$

The index compares the θ_e of the lowest TOVS layer (1000–850 mbar) with the θ_{es} of the third TOVS layer (700–500 mbar).

Based on the observations of 23 island stations and the simultaneous data for January 1983, Khalsa and Steiner (1988) showed that a threshold SI of 0 to 1 is favourable to indicate regions of deep convection; the higher values are non-indicative of convection in the tropical Pacific Ocean.

The SI threshold for deep convection over Arabian Sea was analysed using the available insitu data and is discussed in § 5.

4. Data and analysis

4.1 *Data*

The data used in this study consist of the operational sounding products generated by NESDIS/NOAA of USA. They pertain to the MONEX/FGGE period (1 May through 31 July) from the TIROS-N satellite. These products (about one set in a 2·5° x 2·5° lat-long box) include data on the skin temperature (ST); the 15-layer mean atmospheric temperature profile from 1,000 to 0·4 mbar; and the 3-level total water vapour content (TWVC).

The data used in this analysis from the above set are the skin temperature, atmospheric temperature and water vapour in the 1000–500 mbar altitude region. This information is available in the basic data set as shown in table 1. Besides the above

Table 1. Temperature and water vapour information at different pressure levels (in mbar) as available from NOAA-TOVS.

Level	Layer mean temperature of	Central pressure level	TWVC in the altitude
Surface	Skin	—	—
1st	1000–850	925	1000–700
2nd	850–700	775	
3rd	700–500	600	700–500

data, the cloudiness data provided in the same tape have also been used in this study for purposes of comparison.

4.2 *Calculation of indices*

The results of inversion index ΔT presented here are from our earlier paper and rely only on the data available in the basic NOAA tape.

However, for calculating SI (Khalsa and Steiner 1988), we had to deduce θ_e's at levels where moisture values did not exist in the original NOAA data.

Humidity values are available in the NOAA operational products only at two levels below 500 mbar in contrast to the three levels of temperature values. To obtain the specific humidity corresponding to the 1000–850 mbar level from the 1000–700 and 700–500 mbar-level humidity observations, the following method was employed (Simon and Desai 1986):

As exponential form for vertical distribution of water vapour with a scale height H was assumed. The Newton-Raphson method was employed to iteratively evaluate H from the following relation:

$$W_1/W_2 = \frac{\exp(-Z_{700}/H) - \exp(-Z_{1000}/H)}{\exp(-Z_{500}/H) - \exp(-Z_{700}/H)},$$

where W_1 and W_2 refer to total water vapour content at the two levels provided by TIROS-N satellite (table 1), Z's are the geopotential heights (in km) of the subscripted mbar levels. Considering the coarse vertical resolutions of the temperature and water vapour observations from TOVS, the following approximations were made in the above relation:

$$Z_{1000} = 0{\cdot}0\,\text{km}, \quad Z_{700} = 3{\cdot}0\,\text{km} \quad \text{and} \quad Z_{500} = 5{\cdot}5\,\text{km}.$$

Using the value of H, the water vapour density at surface was evaluated. Further assuming the air density at surface to be 1·2 kg/m^3, the specific humidity (q) at 925 mbar (0·75 km)—the mid-point of the first level temperature information from TOVS—was also obtained.

The relevant potential temperatures were then obtained from the following relations

$$\theta_e(1) = \theta(1)\exp(Lq_{925}/C_pT),$$

where T is the temperature which the parcel at 925 mbar with temperature $T(1)$ and specific humidity q_{925} would have if expanded adiabatically to saturation. Also,

$$\theta_{es}(3) = \theta(3)\exp(Lq_{s,600}/C_pT(3)),$$

where $q_{s,600}$ corresponds to saturation specific humidity at 600 mbar and temperature $T(3)$. In the above expressions L is the latent heat of condensation and C_p the specific heat of air at constant pressure.

4.3 *Spatial and time averaging*

The data at any particular location for any individual day were insufficient for our analysis, mainly due to underlap in the tropical regions of about 8–10 deg in longitude

between successive satellite passes, the other major limitation being the cloud cover which inhibited proper parameter retrievals. Although tempertures could still be retrieved from the microwave sounding unit (MSU) channels, moisture data were lacking in completely cloudy areas. As a result, mean values for moisture variables could be biased toward non-convective conditions over regions with persistent convection.

To help overcome the above limitations we adopted a spatial a 5 × 5 deg lat.-long. grid box) and 5-day time-averaging procedure to investigate the inversion/convection regions over the Arabian sea. These are reasonable considering the spatial and time scales of the monsoon system under study over the Arabian sea.

5. Results and discussion

Here we present the results of the ΔT and SI values for the four important phases (onset, active, break and revival) of 1979 monsoon as also for the pre-monsoon period.

Figure 1 shows the scatter plot of ΔT and SI indices against percentage cloud amount (also available from the NOAA data set) for all the five periods put together. It is seen from figure 1a that for some positive high values of ΔT, the cloud amounts are less. These are over regions where there is no inversion, but no convection either, because of non-availability of moisture. This is the situation during the pre-monsoon periods over the central Arabian sea. Excluding these data points, the increase of cloud amount with increasing ΔT and decreasing SI is very clear from these two figures.

These scatter plots are similar to that of SST and clouds (Graham and Barnett 1987) and the relationship appears to be between maximum cloudiness and the index value with the range of variation in cloudiness for any given value of ΔT and SI being very large. The cloudiness depends on the indices as well as the dynamics. One of these being favourable will be a necessary but not a sufficient condition; this could be one of the reasons for the large spread in the scatter plots observed in figure 1.

Narayanan and Rao (1981) had suggested a threshold of 2°C for ΔT below which inversion was found to exist over the Arabian sea. This was on the basis of comparison with dropsonde in situ observations available during MONEX/FGGE (1979) during the period 1 May to 27 June. From a careful re-examination of figure 1 and other results, we believe that a value of 1°C for ΔT may be more appropriate for the delineation of the inversion over the Arabian sea than 2°C suggested earlier. This also takes into account the observed cloudiness.

For SI threshold also, the dropwindsonde observations available during MONEX (FGGE) were reanalysed. Air temperature, dewpoint temperature, relative humidity and winds were available at many levels generally between 1000 and 400 mbar. Air temperature and dewpoint temperatures (over many layers) corresponding to the two TOVS layers of interest viz 1000–850 mbar and 700–500 mbar were averaged and these observations were used to estimate stability index (SI) as defined earlier.

A total of 85 dropwindsonde profiles over the Arabian sea during May 3–June 27 were considered for comparison. Of these, 25 profiles had a pronounced inversion in the lower levels and 60 profiles showed no inversion in the lower levels. The comparison of SIs independently derived using TOVS and dropwindsonde data showed the following features:

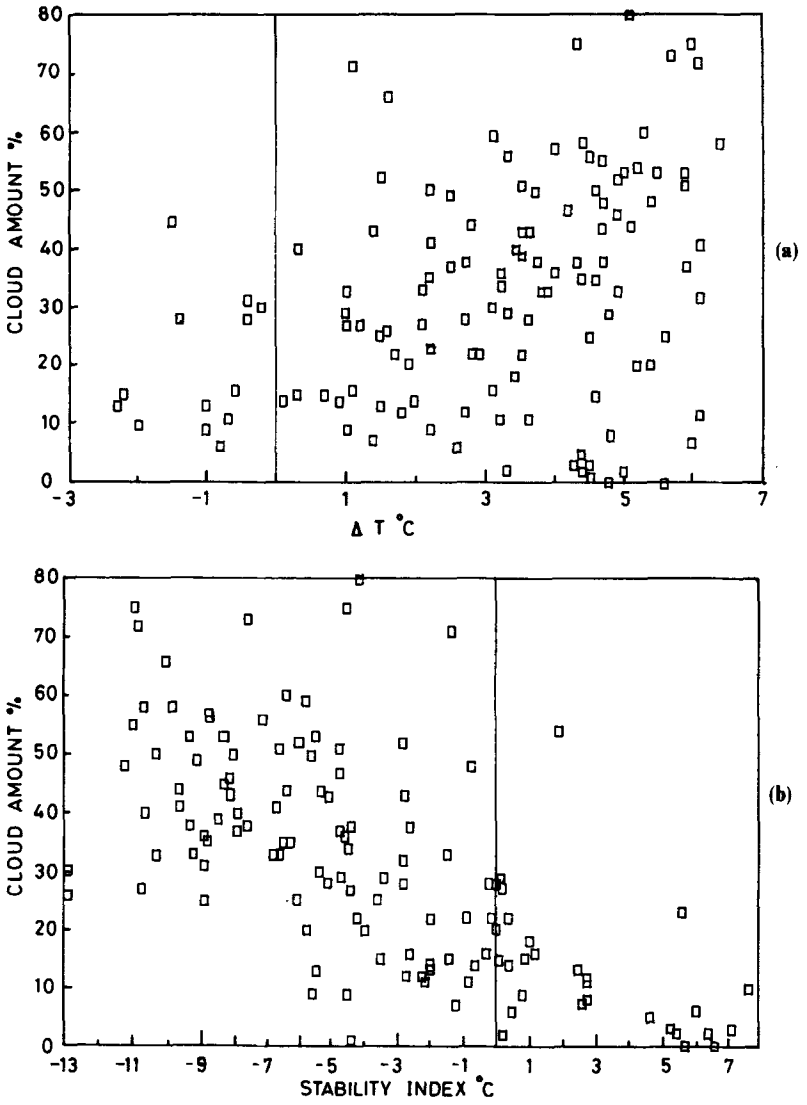

Figure 1. Scatter plots of (a) ΔT *vs* percentage cloudiness. (b) Stability index *vs* percentage cloudiness.

The spot SI comparisons were not satisfactory and showed a large scatter. One of the reasons for this could be the time difference between the satellite and dropsonde observations. However, the spatial distribution of the two SI patterns match satisfactorily. In the case of dropsonde profiles with no inversion, the values of SI for May ranged between + 17 and − 15 and only 2 profiles showed SI greater than − 20 (on May 29). The cloudiness in May ranged between 0 and 40%. On the other hand, 90% of the dropwindsonde 'non-inversion' profiles showed high negative SI values in June ranging between − 10 and − 25 (associated with cloudiness ranging between 40 and 80%), the high negative values corresponding to the active period (22 June). Of the dropsonde profiles having a pronounced inversion at lower levels, SI values ranged

between 0 and + 16, indicating highly stable atmospheric stratifications over the Arabian Sea in May. Appropriately, the associated cloudiness also was < 15%.

With the setting in of the SW monsoon in June the dropsonde-derived SIs (for profiles with inversion) showed a decreasing trend all over the Arabian sea (ranging between − 4 and − 15, with most of them between − 4 and − 9) indicating setting in of favourable conditions for convection but these were certainly much less than the SI values corresponding to non-inversion profiles (of June). Thus the dropsonde derived SIs clearly showed a significant change in the stratification of the lower atmosphere from May to June and also between inversion and non-inversion regions.

In the light of the above analysis carried out in the 5° × 5° spatial and 5-day temporal scale an SI threshold value of − 2 to − 3 was considered indicative of convection. Higher negative values indicate deeper convection. Incidentally Khalsa and Steiner (1988) suggested a SI threshold of 0 to 1°C below which convection was possible over the Pacific.

In the light of these new thresholds we shall examine the next five figures which show the ΔT and SI value maps for the different phases of monsoon. Each grid point (central locations of the 5° × 5° grid) over the sea represents respectively the average ΔT, SI (top line), and the percentage cloud amount (bottom line). For reasons of clarity the number of observations making these averages at each grid point is not shown. In general they range from 5 to 10.

During the pre-onset period (figure 2), the ΔT values are much greater than 1°C all over the Arabian sea indicating absence of inversion. The SI values over the central and northern Arabian sea are also positive and range between + 3 and + 6, which indicate absence of any organized convection. The negative SI values are seen over the eastern Arabian sea (south of 12°N), and also all along 2°N associated with the Inter-Tropical Convergence Zone (ITCZ) where deep convection is quite pronounced. The SI map clearly demarcates the ITCZ and shows the stratification favourable for deep convection associated with ITCZ. The cloud amounts are also seen to be relatively high.

Figure 3 shows the indices map for the onset period (central date: 17 June). The negative SI values are now seen all over the Arabian sea south of 17°N indicating

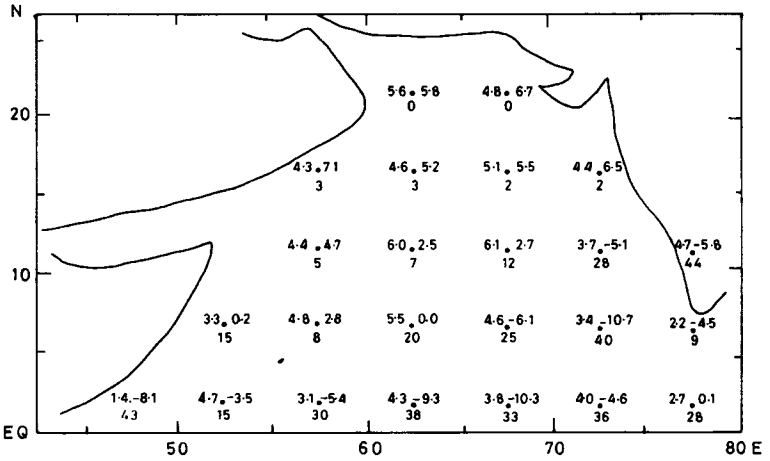

Figure 2. ΔT and SI index map for the premonsoon period (15–19 May 1979).

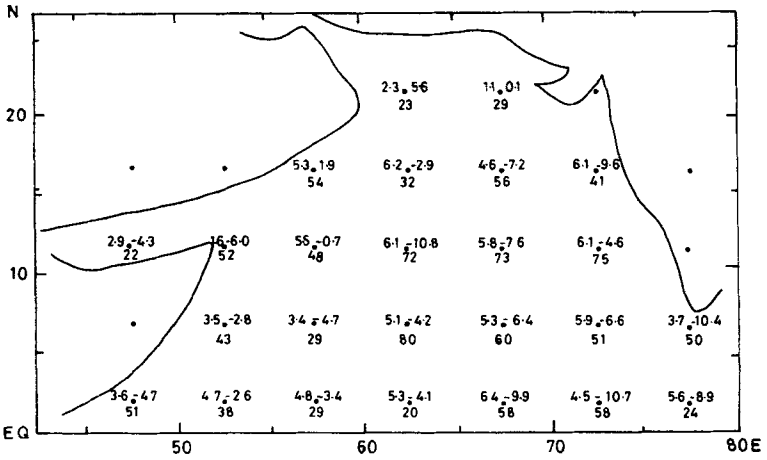

Figure 3. ΔT and SI index map for the onset period (15–19 June 1979).

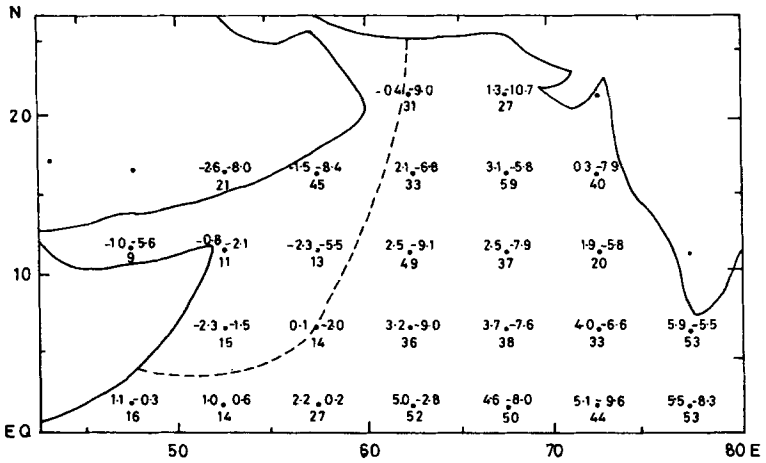

Figure 4. ΔT and SI index map for the active period (25–29 June 1979).

favourable stratification for deep convection associated with the onset of the southwest monsoon. The strong east-west band of negative SI values seems to have moved northwards supporting deep convection. ΔT values are also greater than 1°C all over the Arabian sea. Cloud amounts range from 40 to 80% in many grids. Another notable point is that around 22°N and 60–70°E, two grids of relatively higher values of cloudiness are associated with positive SI. However, ΔT values are of the right order. The overall picture shows satisfactory agreement between the two indices and cloudiness and indicates that monsoon has advanced to about 20°N.

The indices are shown in figure 4 for the active period (27 June). The establishment of the inversion regions, as indicated by ΔT and low cloudiness values, is clearly manifest in the western Arabian sea to the west of 60°E. The figure also shows the extent of the inversion indicated by a dashed line. Higher than 2°C of ΔT are seen over the eastern Arabian sea east of this longitude. The corresponding SI values range between $-5°$ and $-10°$C. These high negative SI values are indicative of highly

unstable atmosphere favourable for deep convection—typical of an active monsoon period. The low negative SI values over the western Arabian sea (south of 15°N) indicate the atmosphere to be less buoyant as compared to the eastern Arabian sea. A few values of negative ΔT's at 17°N in the western Arabian sea are associated with higher cloudiness, and are unexplained. Similarly a few higher negative values of SI at 12°N are associated with lower cloudiness. These anomalies do suggest that both the indices should be considered to account for a proper delineation of the convective activity. All the same a gradual increase (decrease) of ΔT(SI) can be observed from western to eastern Arabian sea for all latitude belts.

For the break monsoon period (figure 5) north of 7°N the ΔT values over the Arabian sea are all less than 1°C (and at two grids range between 1° and 1·5°C) indicating the presence of inversion layers. Compared to the previous period, these inversion regions have moved eastwards and are now seen to encroach the west coast. The corresponding SI values over the north central Arabian sea are all positive indicating an extremely stable atmosphere not favouring deep convection. Over the central Arabian sea (between 7° and 12°N) SI values are negative supporting favourable stratification for deep convection, but they now range only between -1 and -4, considerably lower than during the active period, when these values reached close to -10. It may be noted that Khalsa and Steiner (1988) while examining concurrent satellite (TOVS) and dropsonde measured SI's concluded that higher the negative SI value, lower is the condensation level and higher will be the convection. At west coast north of 17°N, the ΔT values suggest inversion; SI's have low negative values. However, the cloudiness is relatively high. This could be because of the orographic effects and needs a more careful examination.

For the revival period (figure 6) we see that south of 22°N, ΔT values are higher than 1°C. The SI values are low negative west of 60°E. The cloudiness amounts are relatively high (> 20%) all over the Arabian sea east of 55°E. As compared to the break period, it is seen that the SI values over the eastern Arabian sea have considerably increased and now range between -6 and -13, thus clearly indicating the revival of the monsoon. In this particular case the ΔT index seems to perform better than the SI index.

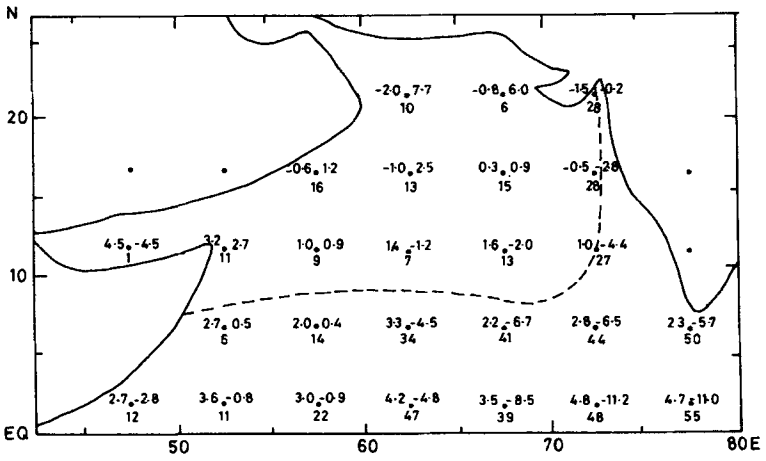

Figure 5. ΔT and SI index map for the break period (3–7 July 1979).

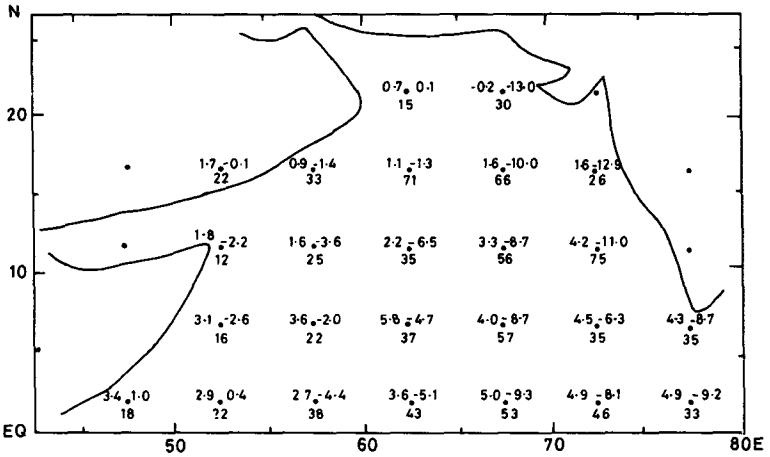

Figure 6. ΔT and SI index map for the revival period (26–30 July 1979).

We have also studied the daily variation of ΔT and SI at two representative boxes centred around 12°N, 62°E and 17°N, 67°E over the Arabian sea during 1 May to 30 July 1979 (figures 7 and 8).

These maps clearly bring out the changes in the stratification of the atmosphere that take place over the Arabian sea with the setting-in of the south west monsoon.

The values of ΔT range between + 3 and + 8 during 1 May to 1 June, indicating the absence of inversions over the Arabian sea; at the same time SI values range between 0 and + 12 indicating that the atmosphere is extremely stable not favouring deep convection. With the setting-in of the south west monsoon, ΔT values show a decreasing trend, but it is associated with dramatic decrease in the SI values and by 15 June, both the boxes acquire negative SI values and this trend continues till 30 July indicating the unstable atmospheric conditions over the Arabian sea favouring deep convection. At the peak of the active period (25 June), the SI values range between − 10° and − 12°C. The associated ΔT values range between 0 and + 1. With the setting in of break conditions around 5 July, the SI values increase significantly and range between 0 and − 2. The revival of the monsoon by 30 July is also clearly seen. The SI map seems to bring out these changes more systematically than the ΔT map. Pre-monsoon period (May) is characterized by high positive SI values depicting stable atmospheric stratifications, while June and July months are associated with high negative SI values indicating extremely unstable atmospheric conditions favouring deep convection over the Arabian sea, which is typical of the monsoon period.

These observations are consistent with the findings of Khalsa and Steiner (1988), that high positive SI values indicate that the atmosphere at low levels is far from saturation and no conceivable amount of lifting will produce deep convection. On the contrary, high negative SI values suggest that the lifting condensation level is quite low and the parcel lifted to midtroposphere will be positively buoyant with respect to its environment and thus unstable.

Thus far in our analysis, we have used the index as suggested by Khalsa and Steiner (1988), which compares the equivalent potential temperature of the lowest layer (1000–850 mbar) with the saturated equivalent potential temperature of the third layer (700–500 mbar), and tried to study the stratifications over the Arabian sea during different phases of monsoon 1979.

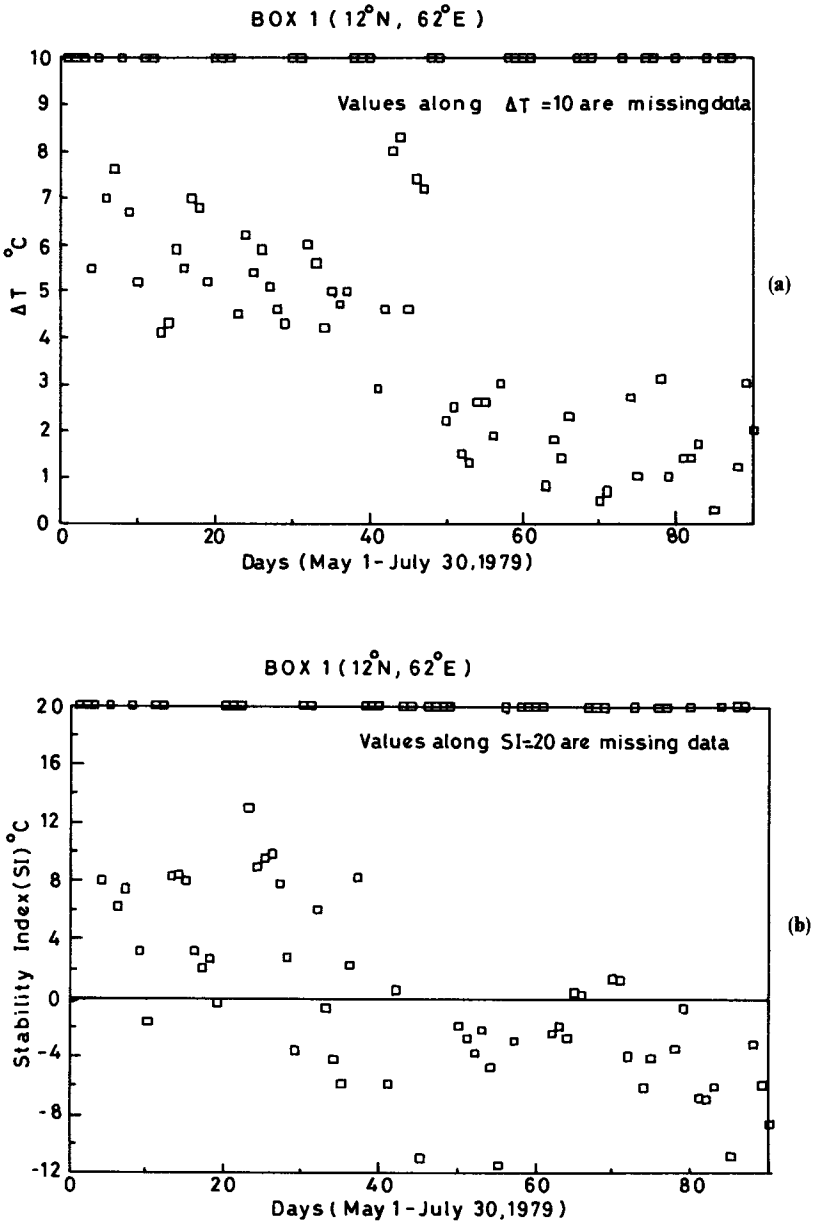

Figure 7. Daily variation of (a) ΔT at box 1, (b) SI at box 1.

The NOAA sounding products produced by NESDIS/NOAA also provide the skin temperature (ST) which we have used in deriving the index for inversion regions (ΔT). Since this skin temperature information is not used in deriving the earlier SI, we have also attempted to derive sets of new stability indices using this information. These indices are defined as

$$\text{SI 1} = \theta_{es}(3) - \theta_e(0),$$

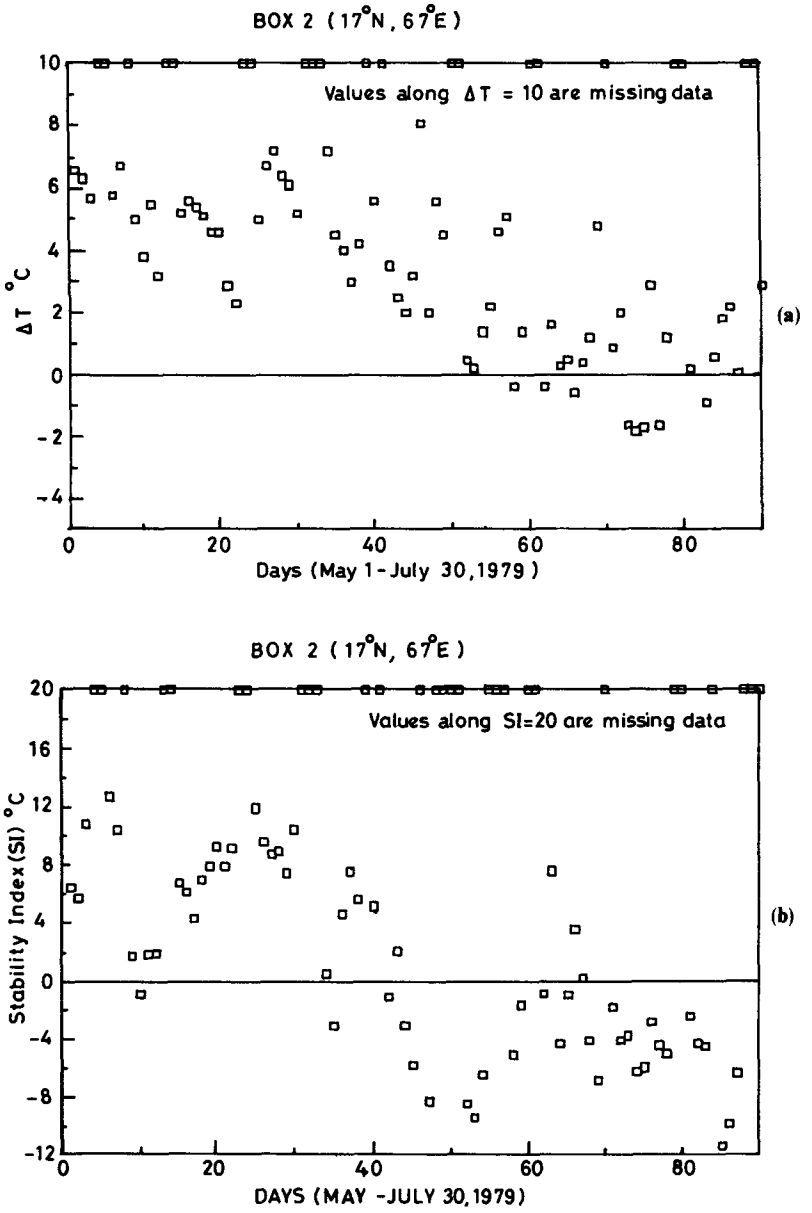

Figure 8. Daily variation of (**a**) ΔT at box 2, (**b**) SI at box 2.

where

$\theta_{es}(3) = \theta_{es}$ at level 3,

$\theta_e(0) = \theta_e$ at surface

and

$$SI2 = \theta_{es}(3) - 0{\cdot}5 \quad (\theta_e(0) + \theta_e(1)),$$

where

$\theta_e(1) = \theta_e$ of the lowest TOVS layer.

The purpose here is to study whether these new stability indices using additional information perform better. For this purpose we have performed regression analysis and calculated the correlation coefficients between ΔT and percentage cloudiness and different SI's and percentage cloudiness. For this all the data for all the monsoon periods were used. These results are given below.

Parameters	Correlation coefficient (r)
ΔT and % cld	0·33
SI and % cld	−0·66
SI 1 and % cld	−0·57
SI 2 and % cld	−0·64

This clearly shows that SI's are better related with percentage cloudiness than ΔT. It also shows that use of the additional information, namely skin temperature (ST), has not resulted in any improvement in the original SI. In fact the correlation coefficient r for SI and percentage cloudiness is −0·66 while the same for SI 1 and percentage cloudiness has reduced to −0·57 and for SI 2 and percentage cloudiness it is −0·64 (which is not significantly different from r for SI and percentage cloudiness). SI 1 which retains the information of SI (apart from using extra $\theta_e(0)$ information) is responsible for this.

Khalsa and Steiner (1988) have also noted that the layer three (700–500 mbar), where the minimum in θ_e and θ_{es} usually occurs, gives the best measure of mid-tropospheric conditions relevant to atmospheric stability. This could be the reason for high correlation between SI and percentage cloudiness.

The NESDIS/NOAA data give rather deep layer averages and are likely to smooth over significant features of the atmospheric profile (e.g. temperature inversions). Another factor which would result in errors in evaluating stability is the lack of moisture data in completely cloudy areas. This could result in a bias of the mean SI values towards non-convective conditions over regions with persistent convection. These are the limitations involved in using TOVS data.

6. Conclusions

Despite the poor vertical resolution of satellite sensors and the various approximations employed, a good correspondence between the two independent indices (ΔT and SI) derived from the operational TOVS sounding products and cloudiness has been established. The shift of the inversion (convection) regions from west (east) to east (west) is seen during different phases of the monsoon, more explicitly by ΔT index than SI. A potential seems to exist for examining the various aspects of monsoon dynamics, including the 30–50 day oscillations, by studying the stability criterion of the atmosphere over a large period from TOVS data through these indices.

Acknowledgements

The authors thank Mr Baby Simon and Mr C M Kishtwal for their help in parts of the analysis.

References

Colon J A 1964 On interactions between the southwest monsoon current and the sea surface over the Arabian sea; *Indian J. Meteorol. Geophys.* **15** 183–200

Ghosh S K, Pant M C and Dewan B N 1978 Influence of the Arabian Sea on the Indian summer monsoon; *Tellus* **30** 117–125

Graham N E and Barnett T P 1987 Sea surface temperature, surface wind divergence and convection over tropical oceans; *Science* **238** 657–659

Khalsa S J S and Steiner E J 1988 A climatology of atmospheric stability for the tropics derived from TOVS; *Third AMS Conf. on Sat. Meteorol and Oceano; Anaheim, Calif*; pp. 7–9

Narayanan M S and Rao B M 1981 Detection of monsoon inversion by TIROS-N satellite; *Nature (London)* **294** 546–548

Philips N, McMillin L, Gruber A and Wark D 1979 An evaluation of early operational temperature soundings from TIROS-N; *Bull. Am. Meteorol. Soc.* **60** 1188–1197

Ramage C S 1966 The summer atmospheric circulation over the Arabian sea; *J. Atmos. Sci.* **23** 144–150

Sen P N and Das H P 1986 Some synoptic aspects of the low level inversions over Arabian sea during MONEX'79 *Mausam* **37** 117–122

Simon B and Desai P S 1986 Equatorial Indian ocean evaporation estimates from operational meteorological satellite and some inferences in the context of monsoon onset; Boundary-Layer *Meteorol.* **37** 37–52